Proc. of the European Safety and Reliability Conference (ESREL 2026)
Edited by José C. Matos, Paulo B. Lourenço, Michael Beer, Daniel Oliveira, Edoardo Patelli, Hélder S. Sousa, Rui A. Silva and Monica Santamaria
 Published by Research Publishing, Singapore.
doi: 10.3850/ESREL2026061419_esrel26-p26313-cd

Resilience Assessment of Green Hydrogen Production Facilities under Escalation Scenarios

Federica Tamburini

LISES – Laboratory of Industrial Safety and Environmental Sustainability - Department of Civil, Chemical, Environmental and Materials Engineering, University of Bologna, Italy. E-mail: federica.tamburini9@unibo.it

Matteo Iaiani

LISES – Laboratory of Industrial Safety and Environmental Sustainability - Department of Civil, Chemical, Environmental and Materials Engineering, University of Bologna, Italy. E-mail: matteo.iaiani@unibo.it

Valerio Cozzani

LISES – Laboratory of Industrial Safety and Environmental Sustainability - Department of Civil, Chemical, Environmental and Materials Engineering, University of Bologna, Italy. E-mail: valerio.cozzani@unibo.it

Green hydrogen production facilities are crucial for low-carbon energy systems but are increasingly exposed to technical, natural, and cyber-physical threats that can evolve into escalation scenarios. In this context, resilience, the ability of a system to anticipate, absorb, respond to, and recover from disruptions while maintaining functionality, is a key property. However, traditional risk assessment approaches mainly focus on failure prevention, neglecting post-failure recovery and adaptation. To address this gap, this study proposes a quantitative, time-dependent framework to assess the resilience of green hydrogen production facilities under escalation scenarios using dynamic Bayesian networks. The model captures the evolving interactions among technical, human, and organizational factors during multiple disruptions. A case study of an alkaline electrolyzer shows that resilience is strongly influenced by escalation mechanisms, as well as by redundancy, monitoring, and safety barriers. Overall, the framework provides a dynamic and integrated perspective to support the design, operation, and management of resilient green hydrogen infrastructures under complex conditions.

Keywords: Resilience assessment, dynamic Bayesian networks, Escalation scenarios, Electrolyzers, Green hydrogen, Energy transition

1. Introduction

Green hydrogen (H_2) production facilities play a key role in decarbonization strategies (Shahzad et al., 2026), yet their integration into digitalized and decentralized energy networks exposes them to new vulnerabilities related to technical failures, human and organizational factors, cyber-physical threats, and external hazards (Iaiani et al., 2023b, Tamburini et al., 2026). Moreover, these systems are prone to escalation scenarios, in which an initial disruption propagates over time, affecting additional equipment and amplifying impacts on overall system performance (Cozzani et al., 2005). Conventional risk assessment approaches primarily emphasize failure prevention or consequence mitigation, often overlooking post-failure recovery and system evolution (Tamburini et al., 2025). As a result, the ability to sustain or restore functionality under degraded conditions may be inadequately represented. These aspects are captured by the concept of resilience, defined as the ability of a system to absorb disturbances, adapt to evolving conditions, and maintain essential functions under both expected and unforeseen stresses (Tong et al., 2020). Consequently, resilience is a key system property for ensuring safe, reliable, and continuous operation. Despite its importance, quantitative methods for assessing resilience under escalation scenarios remain limited, particularly for rapidly evolving energy-transition technologies with scarce long-term operational data (Monie et al., 2025). To address this gap, this study proposes a dynamic, quantitative resilience assessment framework

based on Dynamic Bayesian Networks (DBNs), capable of modeling the time-dependent evolution of system functionality during escalation scenarios (Caetano et al., 2024). The framework leverages DBNs to capture the evolving, probabilistic interactions among technical, human, and organizational factors across multiple disruptions, overcoming the limitations of conventional static approaches. A case study of an alkaline electrolyzer (AEL) system demonstrates the framework's applicability and its potential to support the design and management of resilient green H_2 infrastructures.

2. Methodology

A step-by-step procedure was developed to quantitatively assess system resilience over time in the event of escalation scenarios, as schematized in the flowchart in Fig. *1* and described in the following subsections.

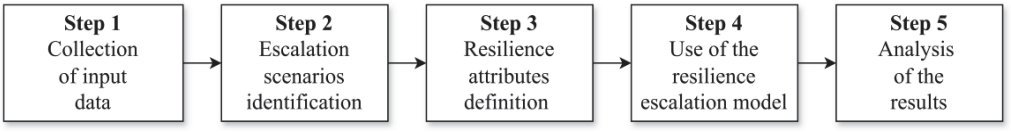

Fig. 1. Flowchart of the methodology developed for resilience assessment.

2.1. *Step 1: Collection of input data*

Step 1 entails the collection of all the input data useful for the assessment. It covers information on the configuration of the engineered system being evaluated, the substances involved, the operating conditions of the equipment, the safety systems and barriers in place, as well as details related to maintenance, inspections, and other specific procedures.

2.2. *Step 2: Escalation scenarios identification*

Step 2 focuses on identifying accident sequences affecting the engineered system, including initiating events, escalation scenarios, and termination actions, together with the safety barriers involved. Hazard identification methods (e.g., HAZOP (BSI, 2016)) support the identification of the first initiating event, hereafter referred to as the first disruption, while barrier failure analysis (e.g., SHIPP methodology (Rathnayaka et al., 2011)) and established techniques (e.g., Bow-Tie analysis (Mannan, 2012)) support the assessment of accident propagation, complemented by additional approaches to account for domino effects (Cozzani et al., 2005). Lastly, the termination phase includes restoration, maintenance, and emergency actions aimed at resolving the accident and restoring system functionality.

2.3. *Step 3: Resilience attributes definition*

Step 3 covers the definition and quantification of the resilience attributes, i.e., absorption, adaptation, restoration, and learning, associated with the events identified in the accident sequences. Absorption represents the system's inherent capability to withstand disruptions through preventive measures; adaptation refers to the ability to recover functionality through internal responses and protection barriers; restoration concerns externally driven actions that restore system operation, including maintenance and emergency interventions; learning reflects the improvement of future responses based on past experience. Except for learning, these attributes depend on the safety barriers activated during accident progression. Their quantification is performed using Fault Tree Analysis (FTA) (Mannan, 2012), which models the causal relationships between root causes and the success or failure of safety barriers. Occurrence probabilities of the fault trees (FTs) are derived from literature (Khakzad et al., 2017, Iaiani et al., 2023a, Tamburini et al., 2024b), technical databases (e.g., OREDA (SINTEF, 2022)), and human reliability analysis (HRA) approaches (Taylor et al., 2017), while learning is treated qualitatively due to its dependence on prior experience.

2.4. *Step 4: Use of the resilience escalation model*

Step 4 applies the developed resilience escalation model to each accident sequence from Step 2. The model consists of four sequential modules, described below, executed in a

predefined order to quantify system resilience. It builds upon the functionality-oriented resilience metric proposed by Tong et al. (2020) for single disruption events. Only the elements essential for this application are summarized; for full details, see Tong et al. (2020).

2.4.1. *Module 1*

Module 1 establishes the functionality states required to evaluate system resilience under escalation conditions. The original metric represents system behavior during a single disruption event with four states: $S1$, the normal operating state with functionality $F1$ at the disruption time t_0; $S2$, the disrupted state with functionality $F2$; $S3$, the adapted state with functionality $F3$ after adaptation; and $S4$, the restored stable state with functionality $F4$ after restoration. To account for multiple escalation scenarios, the original set of states is extended. Let $m = \{1, \dots, M\}$ denote the set of escalation scenarios, with each index j corresponding to a specific scenario affecting the system. For each scenario j, additional states $(S2_j)_{j\in[m]}$, $(S3_j)_{j\in[m]}$, and $(S4_j)_{j\in[m]}$ are introduced to capture the system functionality after the scenario occurs.

2.4.2. *Module 2*

Module 2 adapts Tong et al. (2020)'s metric to include escalation scenarios. Following the original definition, system resilience (R) is the probability that the system remains in, or returns to, a high-functionality state (Tong et al., 2020). This includes the normal operating state $S1$, the recovered state after a single disruption $S4$, and the recovered states for each escalation scenario $(S4_j)_{j\in[m]}$. R is then quantified as the sum of the time-dependent probabilities of these states, computed via DBNs (see Module 4 for details):

$$\mathrm{R} = \mathrm{S1} + \mathrm{S4} + \sum_{\mathrm{j}=1}^{\mathrm{M}} \mathrm{S4}_j \qquad (1)$$

This formulation captures both recovery from a single disruption and additional pathways arising from escalation scenarios.

2.4.3. *Module 3*

Module 3 develops a Markov-chain framework to model the temporal evolution of system functionality under escalation. Building on the functionality states from Module 1, the model extends the single-disruption formulation by allowing transition rates to change after escalation events, capturing variations in resilience attributes (absorption, adaptation, restoration, and learning). Degradation under normal operation is treated as an inherent system property, unaffected by escalation scenarios (TNO, 2005). Failure-related transitions after a disruption are represented using continuous-time Markov chain (CTMC) with memoryless behavior (Serfozo, 2009), modeled through an exponential distribution:

$$\mathrm{P_E}(\lambda_1; \mathrm{t}) = 1 - \mathrm{e}^{-\lambda_1 \mathrm{t}} \qquad (2)$$

where λ_1 is the transition rate under disrupted conditions (inverse of the mean time between system failures, MTBF) and t_0 denotes the time of the first disruption. Adaptation and restoration processes, associated with both internal safety elements and external interventions, are modeled using non-homogeneous CTMCs, as response likelihood increases over time (Trivedi and Bobbio, 2017). Different probability distributions can be employed to model these transition probabilities, including the Weibull distribution or a normal/log-normal distribution, depending on the nature of the process and the available data (TNO, 2005). In the case study, a log-normal distribution is adopted, which better represents the behavior of repair and response times. This formulation applies to both self-recovery (μ_1) and external restoration (μ_2) processes, each defined as the inverse of its respective mean time to repair (MTTR):

$$\mathrm{P_{LN}}(\mu, \delta^2; \mathrm{t}) = 0.5\left(1 + \mathrm{erf}\left(\frac{\ln(\mathrm{t}) - \mu}{\delta\sqrt{2}}\right)\right) \qquad (3)$$

where μ and δ are the mean and standard deviation of the logarithm of the MTTR. System degradation during normal operation is modeled through a simplified constant-rate assumption:

$$\mathrm{P_C}(\lambda_2) = \mathrm{C} \qquad (4)$$

where $\mathrm{C} \in [0,1]$ denotes the level of degradation over time (TNO, 2005). Table 1 shows the transition probabilities of the novel Markov-chain framework for one escalation scenario.

2.4.4. *Module 4*

Module 4 converts the extended Markov chain (see Module 3) into DBNs to assess system

resilience, constructing multiple DBNs to represent the first disruption and subsequent escalation scenarios. DBNs provide a structured and efficient framework to represent time-dependent changes in system functionality (Caetano et al., 2024).

Table 1. Transition probabilities of the novel Markov chain model in case of a single escalation scenario.

Transition rates	**S1**	**S2**	**S3**	**S4**	**$S2_1$**	**$S3_1$**	**$S4_1$**
S1	$1 - P_E(\lambda_1^1, t)$	0	0	0	$P_E(\lambda_1^1, t)$	0	0
S2	0	$1 - P_E(\lambda_1^1, t)$	0	0	$P_E(\lambda_1^1, t)$	0	0
S3	0	0	$1 - P_E(\lambda_1^1, t)$	0	$P_E(\lambda_1^1, t)$	0	0
S4	0	0	0	$1 - P_E(\lambda_1^1, t)$	$P_E(\lambda_1^1, t)$	0	0
$S2_1$	0	0	0	0	$1 - P_{LN}(\mu_1^1, \delta_1^2;\ t)$	$P_{LN}(\mu_1^1, \delta_1^2;\ t)$	0
$S3_1$	0	0	0	0	0	$1 - P_{LN}(\mu_2^1, \delta_2^2;\ t)$	$P_{LN}(\mu_2^1, \delta_2^2; t)$
$S4_1$	$P_C(\lambda_2)$	0	0	0	0	0	$1 - P_C(\lambda_2)$

Each DBN includes six nodes, "First Disruption / Escalation Scenario", "State of Functionality", "Absorption", "Adaptation", "Restoration", and "Learning", alongside "Contributing Element" nodes associated with resilience attributes. Root nodes comprise the "First Disruption / Escalation Scenario", "Learning", and a subset of the "Contributing Element" nodes (i.e., the root causes), while "State of Functionality" acts as the leaf node. Intermediate nodes consist of the resilience attributes nodes and the remaining "Contributing element" nodes, with arcs representing causal relationships. System functionality evolves as a function of the current event (first disruption or escalation scenario), resilience attributes, and prior system states, capturing both disruption effects and the natural time-dependent degradation. All temporal dependencies are modeled as first-order, influencing only neighboring time steps. Node states are assigned as follows: "State of Functionality" has four or more states depending on escalation scenarios, "First Disruption / Escalation scenario" and "Learning" are binary (YES / NO); "Absorption", "Adaptation", and "Restoration" are expressed as HIGH / LOW; and "Contributing Element" as SUCCESS / FAILURE, based on the status of the associated root causes or Boolean FTA logic. Each node is quantified via conditional probability tables (CPTs), with marginal probabilities for root nodes and conditional probabilities for intermediate and leaf nodes. Two CPTs are used for "State of Functionality" node: one for the initial condition and one for subsequent time steps, derived from the Markov chain transition probabilities. In contrast, all other nodes use a single CPT. The CPT of the "First Disruption" node is defined through marginal probabilities, typically fixing the occurrence of the initial event to analyze post-accident system behavior, while the CPT of the "Learning" node reflects the degree of available past experience. Conversely, CPTs associated with "Escalation scenario" nodes are conditionally specified based on the states of their parent nodes, so that escalation probabilities emerge from the underlying triggering mechanisms rather than from marginal assignment. CPTs for "Contributing element" nodes follow marginal probabilities for root nodes and Boolean logic for non-root nodes, while CPTs for resilience attribute combine contributions from all parent nodes equally. DBNs are solved sequentially using GeNIe Modeler (BayesFusion, 2026), producing time-dependent functionality curves that are combined over their respective intervals

to obtain the overall resilience curve, according to the metric defined in Module 2.

2.5. *Step 5: Analysis of the results*

Step 5 analyzes the generated resilience curve to evaluate system recovery times, identify design improvements, and support further investigations (e.g., posterior analysis, sensitivity analysis).

3. Case study

This section describes the case study and provides the input data required for **Step 1** of the methodology. The case study considers a green H_2 production plant injecting H_2 into an existing natural gas network at 70 bara. The facility has two parallel production lines, each composed of ten 1 MW AEL modules and a dedicated conditioning section. Electrolyzers use an aqueous potassium hydroxide electrolyte, producing about 20 kg/h of H_2 with gas–liquid separation units for water recovery and recirculation. The downstream conditioning sections include cooling and water removal units, an oxygen removal reactor, and a compressor train to reach the delivery pressure. Safety is ensured by an Emergency Shutdown (ESD) system triggered by fire or smoke and Local Shutdown (LSD) systems for the electrolyzers and conditioning lines, activated under hazardous conditions or manually from the control room.

4. Results and discussion

This section presents the application of the proposed methodology to the case study, focusing on Steps 2 to 5 based on the input data (Step 1) provided in Section 3.

Step 2 consisted of applying the SHIPP methodology (Rathnayaka et al., 2011) to identify the accident sequence, while escalation scenarios were evaluated according to Cozzani et al. (2005). The first disruption comprised a gaseous H_2 release from a water removal separator (located in the conditioning line) through a 5 mm hole, with a release rate of 0.029 kg/s. Since the inlet flow rate was 0.072 kg/s, the release was continuously fed, and immediate ignition was assumed due to H_2's wide flammability range and low minimum ignition energy, resulting in a jet-fire at time t_0 (Tamburini et al., 2024a). The ESD and sprinkler systems were assumed to fail after 5 and 10 min, respectively, while manual firefighting actions were considered insufficient to prevent escalation. Prolonged thermal radiation from the jet-fire, although not directly impinging on nearby equipment on the parallel conditioning line, was assumed to cause structural failure after 20 min (based on time-to-failure thresholds and PHAST consequence modelling (DNV, 2025)), leading to a fireball as the escalation scenario. The analysis accounted for safety barriers identified by SHIPP (Rathnayaka et al., 2011), namely Release Prevention Barriers (RPBs), Release Detection Barriers (RDBs), Ignition Prevention Barriers (IPBs), and Escalation Prevention Barriers (EPBs), which were used to defined resilience attributes in Step 3 and to support the DBN modeling.

Step 3 consisted of defining and quantifying resilience attributes using FTs based on the identified safety barriers. Absorption reflected preventive measures captured by RPB and IPB FTs, adaptation corresponded to mitigative barriers related to RDBs and EPBs, and restoration accounted for external interventions and site-specific responses not fully represented through FTs. The quantification was performed by assigning occurrence probabilities to the root causes of the FTs using data from Khakzad et al. (2017), Taylor et al. (2017), SINTEF (2022), Iaiani et al. (2023a) and Tamburini et al. (2024b) (see Table 2). Emergency maintenance was treated separately, with a failure probability of 4.00×10^{-2} (Ibrahim et al., 2019), representing restoration actions external to the system.

Table 2. Failure probabilities of the root causes considered in the case study.

Tag	Root cause	Probability
X1	External fire	1.54×10^{-4}
X2	PSV failure	2.12×10^{-5}
X3	Inadequate inspection and testing procedures	2.00×10^{-2}
X4	Error in manual inspection	9.82×10^{-3}
X5	Design failure	1.44×10^{-2}
X6	Lighting	3.40×10^{-2}
X7	Malicious intervention	2.80×10^{-4}
X8	Inadequate control system	5.00×10^{-2}
X9	Inadequate maintenance	5.00×10^{-2}
X10	Inadequate supervision	3.40×10^{-2}
X11	Inadequate training	2.50×10^{-2}
X12	ESD sensors failure	2.74×10^{-1}

Table 2 (Continued)

X13	Automatic ESD valves failure	1.17×10^{-1}
X14	H_2 sensors failure	7.54×10^{-3}
X15	H_2 alarm failure	2.52×10^{-3}
X16	Human error	4.77×10^{-2}
X17	Pressure gauge failure	1.54×10^{-4}
X18	Lightning protection issues	3.94×10^{-3}
X19	Static sparks from operators	1.25×10^{-1}
X20	Static sparks from equipment	3.31×10^{-3}
X21	Electrical sparks	3.06×10^{-3}
X22	Spark inhibitors shield issues	4.00×10^{-2}
X23	Fire suppression system failure	5.58×10^{-2}
X24	Firefighting actions failure	9.02×10^{-2}
X25	Flame alarm failure	2.10×10^{-2}
X26	Ignition detection failure	2.53×10^{-1}
X27	Manual fire alarm failure	5.00×10^{-2}
X28	Smoke alarm failure	2.10×10^{-2}
X29	Smoke detection sensors failure	7.41×10^{-2}

Step 4 consisted of developing, quantifying, and implementing two DBNs, one for each accidental event identified in Step 2, using GeNIe Modeler (BayesFusion, 2026). The first DBN modeled the H_2 release leading to a jet-fire (first disruption, Fig. 2), while the second represented the consequent fireball (escalation scenario, Fig. 3). In the first DBN, the event node was set to "occurred", and the "Learning" node accounted for the influence of prior experience on system recovery. Root contributing elements were populated using the marginal probabilities of the root causes derived in Step 3, and the CPTs of intermediate nodes were obtained by translating the Boolean logic of the FTs into the DBN framework. The escalation scenario was not modeled as an independent root event; its occurrence depended on the failure of the ESD at 5 min and the sprinkler system at 10 min, introduced as evidence nodes in the second DBN, thus resulting from the propagation of previously observed failures. System functionality was modeled through discrete states using a Markovian approach with degradation-dependent transition rates, as reported in Table 3 for the first disruption and Table 4 for the escalation scenario. Failure, repair, and degradation processes were described using exponential, log-normal, and constant distributions, respectively.

Table 3. Transition rates - first disruption.

Transition rates	Unit	H	L
$\boldsymbol{\lambda_1}$	min^{-1}	0.002	0.003
μ_1	min^{-1}	0.2	0
μ_2	min^{-1}	0.022	0
$\boldsymbol{\lambda_2}$	min^{-1}	0.001	0.001

Table 4. Transition rates - escalation scenario.

Transition rates	Unit	H	L
$\boldsymbol{\lambda_1^1}$	min^{-1}	2	3.03
μ_1^1	min^{-1}	0.1	0
μ_2^1	min^{-1}	0.006	0
$\boldsymbol{\lambda_2}$	min^{-1}	0.001	0.001

Step 5 consisted of simulating the DBNs and driving the dynamic resilience curve across the two accidental events.

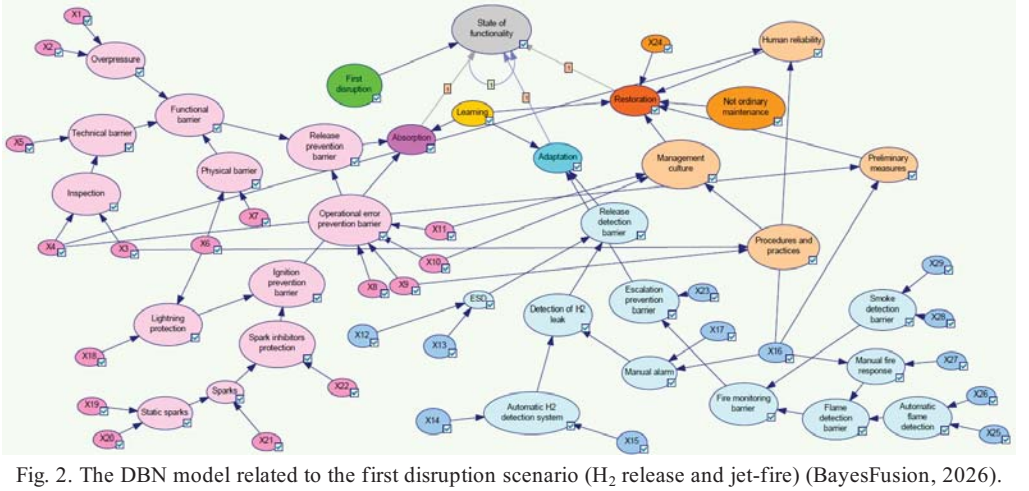

Fig. 2. The DBN model related to the first disruption scenario (H_2 release and jet-fire) (BayesFusion, 2026).

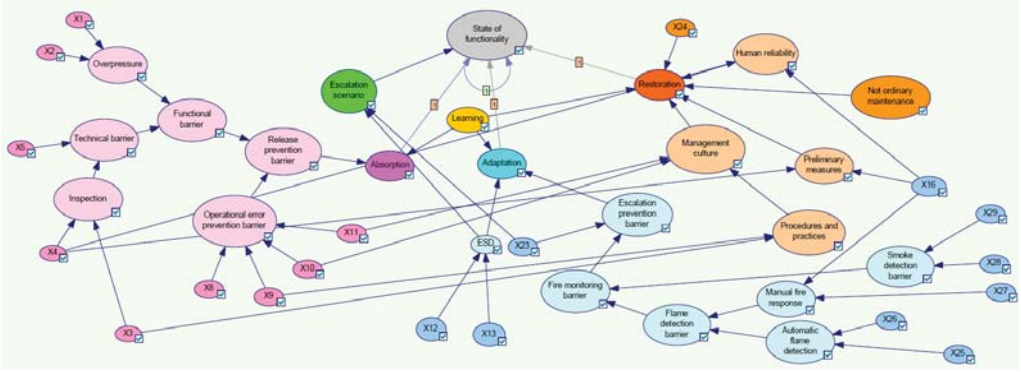

Fig. 3. The DBN model related to the escalation scenario (catastrophic rupture and fireball) (BayesFusion, 2026).

The DBN associated with the first disruption was simulated over a 20-min time horizon, corresponding to the time required for jet-fire exposure to cause structural failure of the secondary equipment. The escalation DBN was then activated at 20 min and simulated until functional stabilization was achieved. Regarding restoration, firefighting actions were assumed to be already ongoing at the time of fireball occurrence, with no additional delay for arrival or mobilization. The analysis focused on accident mitigation rather than full system restoration, and complete functionality was defined as the mitigation of both scenarios, excluding equipment replacement. Results were used to derive the dynamic resilience curve across the two accidental events (see Fig. 4).

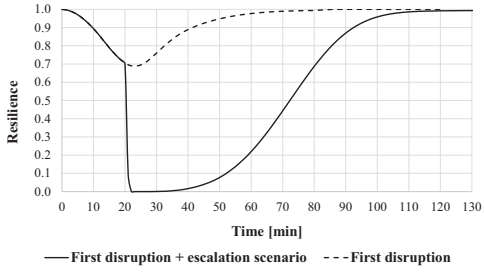

Fig. 4. Calculated resilience curve.

The dashed curve in Fig. 4 corresponds to the first disruption only. Resilience initially drops but remains above 0.7, indicating that preventive and mitigative measures maintain system functionality. In other words, the plant operates on the second conditioning line at reduced capacity. Around 60 min, resilience stabilizes near 1 due to containment actions and effective safety barriers, showing a steady recovery without further escalation. The solid curve in Fig. 4 denotes the first disruption combined with the escalation scenario. Here, resilience drops sharply around 20 min when the jet-fire causes structural failure of secondary equipment and generates a fireball, nearly reaching 0. Now, both conditioning lines are damaged, halting plant operation. Recovery is gradual, driven by safety barriers and restoration measures, reaching 1 at 110 min. The curve difference highlights the significant impact of the escalation scenario and confirms that the jet-fire exposure time to secondary equipment is vital. In addition, Fig. 4 points out the role of conditioning-line redundancy and proper ESD and sprinkler maintenance in preventing total functionality loss.

5. Conclusions

A dynamic DBN-based framework was developed to assess resilience in a green H_2 production facility under escalation scenarios, considering a jet-fire followed by a fireball. The case study showed that preventive and mitigative measures maintain system functionality during minor disruptions, whereas escalation scenarios cause sharp drops and prolong recovery. Key drivers of resilience include exposure time, barrier reliability, and restoration rates. Outcomes depend on modeling assumptions: memoryless CTMCs simplify implementation but ignore path-dependent degradation, and transition rates relay on literature rather than plant-specific data, so values are scenario-based and mainly comparative. This is partly due to the limited availability of long-term failure data for

emerging green H_2 facilities, though real operational data can also be obtained from monitoring, maintenance records, and expert judgment. Finally, assumptions regarding restoration-time distributions affect the depth and evolution of the resilience curve. The framework can be extended to multiple interacting escalations, yet complexity increases state-space size and parameter uncertainty. Overall, this approach complements traditional static risk assessments by capturing time-dependent system evolution and recovery, supporting the design of resilient H_2 infrastructures. In practice, it helps operators select mitigation measures, plan maintenance, and develop contingency strategies to enhance resilience.

Acknowledgement

This work was supported by the Italian Ministry of University and Research under the National Recovery and Resilience Plan (Project "Network 4 Energy Sustainable Transition", PE00000021, CUP J33C22002890007) and the ELVHYS project (No. 101101381) under the Clean Hydrogen Partnership - EU. UK participants were supported by UKRI (Grant Nos. 10063519 and 10070592).

References

BayesFusion. (2026). GeNIe Modeler (v. 5.0) [Software].

British Standards Institution (BSI). (2016). Hazard and operability studies (HAZOP): Application guide. BSI.

Caetano, H. O., Neto, L. D., Fogliatto, M. S. S., and Maciel, C. D. (2024). Resilience assessment of critical infrastructures using dynamic Bayesian networks and evidence propagation. *Reliability Engineering & System Safety*, 241, 109691.

Cozzani, V., Gubinelli, G., Antonioni, G., Spadoni, G., and Zanelli, S. (2005). Domino effect risk in quantitative area risk analysis. *Journal of Hazardous Materials*, 127, 14–30.

DNV. (2025). PHAST (v. 9.11) [Software].

Iaiani, M., Tugnoli, A., and Cozzani, V. (2023a). Cyber-risk identification for control and safety systems. *Process Safety and Environmental Protection*, 172, 69–82.

Iaiani, M., Tugnoli, A., and Cozzani, V. (2023b). Process hazard and operability analysis of BPCS and SIS malicious manipulations by POROS 2.0. *Process Safety and Environmental Protection*, 176, 226–237.

Ibrahim, H., and Patruni, J. R. (2019). Bayesian network analysis of fire safety barriers in floating LNG facilities. *SN Applied Sciences*, 1, 1–17.

Khakzad, S., Khan, F., Abbassi, R., and Khakzad, N. (2017). Accident risk-based life cycle assessment for fuel selection. *Process Safety and Environmental Protection*, 109, 268–287.

Mannan, S. (2012). *Lees' loss prevention in the process industries*. Elsevier.

Monie, S. W., Gustafsson, M., Önnered, S., and Guruvita, K. (2025). Renewable and integrated energy system resilience – A review and generic resilience index. *Renewable and Sustainable Energy Reviews*, 215, 115554.

Rathnayaka, S., Khan, F., and Amyotte, P. (2011). SHIPP methodology: Predictive accident modeling approach. Part I. *Process Safety and Environmental Protection*, 89, 151–164.

Serfozo, R. (2009). *Continuous-time Markov chains*. In Applied stochastic processes, pp. 241–242. Springer.

Shahzad, S., Alrumayh, O., Almutairi, A., and Altamimi, A. (2026). Green hydrogen: A review of technological innovations, economic viability, and global prospects. *Renewable and Sustainable Energy Reviews*, 225, 116162.

SINTEF. (2022). OREDA: Offshore and onshore reliability data. SINTEF.

Tamburini, F., Iaiani, M., and Cozzani, V. (2025). Analysis of system resilience in escalation scenarios involving LH_2 bunkering operations. *Reliability Engineering & System Safety*, 257, 110816.

Tamburini, F., Kluge, M., Habib, A. K., Ustolin, F., Cozzani, V., and Paltrinieri, N. (2024a). Exploring experimental tests concerning liquid hydrogen releases. *Process Safety and Environmental Protection*, 192, 1330–1343.

Tamburini, F., Ustolin, F., Cozzani, V., and Paltrinieri, N. (2024b). Safety barrier performance in liquid hydrogen bunkering. *Proc. ASME OMAE2024*, pp. 1–9.

Tamburini, F., Wismer, S. E., Cozzani, V., and Groth, K. M. (2026). Bayesian network model for assessing hydrogen ignition probability. *Reliability Engineering & System Safety*, 268, 111959.

Taylor, C., Øie, S., and Paltrinieri, N. (2017). Human reliability in the petroleum industry: Petro-HRA. *Proc. ESREL 2016*, p. 162.

TNO. (2005). Red Book: Probability methods. TNO.

Tong, Q., Yang, M., and Zinetullina, A. (2020). A dynamic Bayesian network-based approach to resilience assessment of engineered systems. *Journal of Loss Prevention in the Process Industries*, 65, 104152.

Trivedi, K. S., and Bobbio, A. (2017). *Non-homogeneous continuous-time Markov chains*. Reliability and Availability Engineering, 489–508.